

## Distortion Effects in $d + \alpha$ System\*†

D. R. Thompson and Y. C. Tang

*School of Physics, University of Minnesota, Minneapolis, Minnesota 55455*

(Received 28 February 1973)

The deuteron specific distortion effect in the  $d + \alpha$  problem is considered with a microscopic procedure. This procedure consists in the addition of square-integrable or distortion functions into the usual no-distortion resonating-group wave function. The result shows that with the consideration of this effect, a nucleon-nucleon potential which fits the low-energy two-nucleon scattering data and which yields a satisfactory agreement with the empirical  $\alpha + \alpha$  phase shifts can be used to describe quite well the  $d + \alpha$  experimental data. Also, it is shown that the specific distortion effect has an odd-even character; it has significant effects in even- $l$  states, but not in odd- $l$  states. Resonance structures are found in the partial-wave scattering amplitudes. These structures arise as a consequence of the coupling of the compound-nucleus states with the elastic scattering channel.

### I. INTRODUCTION

In a series of investigations,<sup>1</sup> we have examined the scattering of two light nuclei  $A$  and  $B$  with the resonating-group method in the one-channel no-distortion approximation. In this approximation, the wave function describing the system is assumed as

$$\Psi_0 = \mathcal{Q}[\phi_A \phi_B F(\vec{r}_A - \vec{r}_B) \xi(s, t)], \quad (1)$$

where  $\mathcal{Q}$  is an antisymmetrization operator,  $\phi_A$  and  $\phi_B$  describe the internal spatial behavior of the two nuclei  $A$  and  $B$ , respectively, and  $\xi$  is an appropriate spin-isospin function. The function  $F(\vec{r})$ , which describes the relative motion between the two nuclei, is determined from the variational equation

$$\langle \delta \Psi_0 | H - E' | \Psi_0 \rangle = 0, \quad (2)$$

with  $H$  being the many-nucleon Hamiltonian operator, given by

$$H = -\frac{\hbar^2}{2M} \sum \nabla_i^2 + \sum V_{ij}, \quad (3)$$

and  $E'$  being the total energy, composed of the internal energies of the two nuclei and the relative energy  $E$  in the c.m. system. The quantity  $V_{ij}$ , which represents the nucleon-nucleon potential, is chosen to yield correct values for the effective-range parameters and is of the form

$$V_{ij} = \left( \frac{1+P_{ij}^\sigma}{2} V_t + \frac{1-P_{ij}^\sigma}{2} V_s \right) \times \left( \frac{u}{2} + \frac{2-u}{2} P_{ij}^r \right) + \frac{1+\tau_{iz}}{2} \frac{1+\tau_{jz}}{2} \frac{e^2}{r_{ij}}, \quad (4)$$

where  $V_t$  and  $V_s$  are the  $s$ -wave triplet and singlet potentials, respectively. The quantity  $u$ , which will be called the exchange-mixture parameter, cannot be precisely determined from the nucleon-

nucleon scattering data, since the potential of Eq. (4) does not contain a noncentral component. However, the experimental observation that the neutron-proton differential scattering cross section is about symmetrical with respect to  $90^\circ$  does indicate that the exchange mixture should be of a near-Serber type, i.e., the value of  $u$  should be close to 1.

Using Eqs. (1)–(4), it can be easily shown that the resultant equation satisfied by  $F(\vec{r})$  is of the form

$$\left[ \frac{\hbar^2}{2\mu} \nabla^2 + E - V_D(r) - V_C(r) \right] F(\vec{r}) = \int K(\vec{r}, \vec{r}') F(\vec{r}') d\vec{r}', \quad (5)$$

where  $\mu$  is the reduced mass,  $V_D$  is the direct nuclear potential,  $V_C$  is the direct Coulomb potential, and  $K(\vec{r}, \vec{r}')$  is the kernel function for the nonlocal interaction between  $A$  and  $B$ , arising from the exchange character in the nucleon-nucleon potential and the antisymmetrization procedure. If we further introduce into Eq. (5) a phenomenological imaginary potential to take approximate account of reaction effects and adopt an adjustment procedure to be discussed in the next paragraph, then our calculations<sup>2</sup> showed that the one-channel no-distortion resonating-group method can yield an adequate description of the scattering processes in all cases we have so far examined.

Especially in systems involving two light nuclei, one might expect that effects due to mutual distortion of the two scattering nuclei in the strong-interaction region may not be unimportant. In our previous calculations where a trial wave function of the type given by Eq. (1) was adopted, these effects were partially taken into account by the presence of the antisymmetrization operator

(Pauli- or exchange-distortion effects). However, there may be additional distortion effects (specific distortion effects) which still need to be considered in a proper description of the scattering problem. Therefore, in all our previous studies,<sup>1,2</sup> we have made a rather crude compensation of these specific distortion effects by choosing for each scattering system a value of  $u$  in Eq. (4) which yielded a best agreement with the experimental data in that particular system. The rationale for adopting such a procedure was as follows. One expects that specific distortion effects will create an additional attractive interaction<sup>3</sup> between the two nuclei and, therefore, a phenomenological variation of the potential  $V_D$  in Eq. (5), which becomes more attractive as the value of  $u$  increases, may simulate the contribution due to these effects. In addition, it should be noted that an adjustment in  $u$  does have the advantage that it leaves the values of the nucleon-nucleon effective-range parameters unchanged.

The above-mentioned procedure has led to  $u$  values of 0.92 for  $\alpha + \alpha$  scattering,<sup>4</sup> 1.1 for  $d + {}^3\text{H}$  scattering,<sup>5</sup> and 1.2 for  $d + d$  scattering.<sup>6</sup> In the case of  $\alpha + \alpha$  scattering, a brief examination by Niem, Heiss, and Hackenbroich<sup>7</sup> has shown that specific distortion effects have relatively minor influence on the scattering phase shifts. Thus the finding of rather large values of  $u$  in the  $d + d$  and  $d + {}^3\text{H}$  cases is an indication that when a deuteron, or even a triton, is involved in a scattering problem, specific distortion effects do have significant consequences.

Even though the procedure of adjusting the exchange-mixture parameter  $u$  has yielded rather successful comparisons between calculations and experiments,<sup>1,2</sup> it is certainly rather undesirable, since it introduces a phenomenological aspect into an otherwise microscopic calculation. A much more desirable way to take specific distortion effects into account would be to improve the no-distortion approximation by introducing more freedom into the trial wave function of Eq. (1) in the region of strong interaction. Such a procedure has, in fact, been proposed and briefly tested by Jacobs *et al.*<sup>8</sup> and will be considered in detail in this investigation.

In this study, we shall consider the problem of  $d + \alpha$  scattering as an example. The reason for choosing this particular problem for a detailed examination is as follows. Because of the rigidity of the  $\alpha$  particle, it is allowable, as a good approximation, to neglect the distortion of the  $\alpha$  particle in the interaction region of the two clusters. The major effect in this system should be that due to the specific distortion of the deuteron cluster. For this latter cluster, it has been

shown<sup>6</sup> that the use of a three-Gaussian wave function, with the parameters determined variationally by minimizing the expectation value of the deuteron Hamiltonian, can yield a good agreement with the experimental results in both the binding energy, the rms radius, and the charge form factor. As a consequence, it can be expected that the compressibility of the deuteron cluster will be given accurately and the results of this study should reflect the nature of the deuteron distortion effects in a fairly reliable way.

The procedure we use is to augment the wave function of Eq. (1) by a sum of square-integrable functions with linear variational amplitudes. Each of these square-integrable or distortion functions has also a  $d + \alpha$  cluster structure, but with the deuteron cluster chosen to have a rms radius either larger or smaller than that of a free deuteron. By using a variational method, we then determine the linear amplitudes of these distortion functions, together with the scattering function  $F(\vec{r})$ . In this way, we shall show that specific distortion effects can be properly taken into account and a value of  $u$  close to that determined from  $\alpha + \alpha$  scattering can be used to explain the experimental  $d + \alpha$  scattering and bound-state results.

We should mention that Jacobs, Wildermuth, and Wurster<sup>9</sup> have used the same method to examine the  $d + \alpha$  problem. They have, however, considered the distortion effects only in the  $l = 0$  partial wave and have employed, for simplicity, a single distortion function. In the present calculation, we shall extend their calculation to include many partial waves and to examine the convergence problems in this method by the use of a large number of distortion functions.

In Sec. II, a formulation of the problem is described. Section III is devoted to a detailed discussion of the choice of nonlinear parameters in the distortion functions. Results for the scattering phase shifts and  ${}^6\text{Li}$  compound-nucleus resonances are given in Sec. IV. Finally, in Sec. V, discussions and concluding remarks are made.

## II. FORMULATION

In this section, we discuss the formulation of the  $d + \alpha$  problem, with deuteron specific distortion effects taken into account. As was mentioned in the Introduction, this will be achieved by the addition of square-integrable or distortion functions into the no-distortion approximation. That is, we assume the trial function to have the form

$$\Psi_N = \mathcal{G}[\phi_\alpha \phi_d F(\vec{r}) \xi(s, t)] + \sum_{i=1}^N \mathcal{G}[\phi_\alpha \phi_i G_i(\vec{r}) \xi(s, t)], \quad (6)$$

where  $N$  is the number of distortion functions and  $\vec{r} = \vec{r}_\alpha - \vec{r}_d$ , with  $\vec{r}_\alpha$  and  $\vec{r}_d$  being the position vectors of the center of mass of the  $\alpha$  and the deuteron clusters, respectively. The function  $\phi_\alpha$  describes the spatial structure of the  $\alpha$  particle and is assumed as

$$\phi_\alpha = \exp\left[-\frac{1}{2}\alpha \sum_{i=1}^4 (\vec{r}_i - \vec{r}_\alpha)^2\right]. \quad (7)$$

The width parameter  $\alpha$  is chosen to yield the experimentally determined value of the rms radius of the nucleon distribution in  ${}^4\text{He}$ ; it is given by

$$\alpha = 0.514 \text{ fm}^{-2}, \quad (8)$$

which corresponds to a rms radius of 1.48 fm. The deuteron internal function  $\phi_d$  is chosen to be

$$\phi_d = \sum_{i=1}^3 A_i \exp\left[-\frac{1}{2}\alpha_i \sum_{j=5}^6 (\vec{r}_j - \vec{r}_d)^2\right], \quad (9)$$

with the parameters determined by minimizing the expectation value of the deuteron Hamiltonian. These parameters are<sup>6</sup>

$$\begin{aligned} A_1 &= 1.0, & \alpha_1 &= 0.07284 \text{ fm}^{-2}, \\ A_2 &= 3.631, & \alpha_2 &= 0.3657 \text{ fm}^{-2}, \\ A_3 &= 5.746, & \alpha_3 &= 1.4696 \text{ fm}^{-2}. \end{aligned} \quad (10)$$

The functions  $\phi_i$  and  $G_i$  in the distortion-function term of  $\Psi_N$  are assumed to have the forms

$$\phi_i = \exp\left[-\frac{1}{2}\tilde{\alpha}_i \sum_{j=5}^6 (\vec{r}_j - \vec{r}_d)^2\right] \quad (11)$$

and

$$G_i = \sum_{l=0}^{\infty} \tilde{A}_{li} \frac{g_{li}(r)}{r} P_l(\cos\theta), \quad (12)$$

with

$$g_{li}(r) = r^{n+1} \exp\left(-\frac{2}{3}\tilde{\beta}_i r^2\right). \quad (13)$$

The values of  $n$  in Eq. (13) are chosen in the following way:

$$\begin{aligned} n &= 2, & \text{for } l &= 0, \\ n &= 3, & \text{for } l &= 1, \\ n &= l, & \text{for } l &\geq 2. \end{aligned} \quad (14)$$

The rationale for choosing these particular values of  $n$  has been given previously<sup>9</sup> and will not be repeated here.

The relative-motion function  $F(\vec{r})$  and the linear variational amplitudes  $\tilde{A}_{li}$  will be determined by solving the equation

$$\langle \delta \Psi_N | H - E' | \Psi_N \rangle = 0, \quad (15)$$

with  $H$  being the Hamiltonian operator, given by

$$H = -\frac{\hbar^2}{2M} \sum_{i=1}^6 \nabla_i^2 + \sum_{i>j=1}^6 V_{ij}. \quad (16)$$

In the above equation, the quantity  $V_{ij}$  is the two-nucleon potential of Eq. (4); it has

$$\begin{aligned} V_t &= -V_{0t} \exp(-\kappa_t r^2), \\ V_s &= -V_{0s} \exp(-\kappa_s r^2), \end{aligned} \quad (17)$$

with

$$\begin{aligned} V_{0t} &= 66.92 \text{ MeV}, & \kappa_t &= 0.415 \text{ fm}^{-2}, \\ V_{0s} &= 29.05 \text{ MeV}, & \kappa_s &= 0.292 \text{ fm}^{-2}. \end{aligned} \quad (18)$$

As for the choice of the set of nonlinear parameters  $\tilde{\alpha}_i$  and  $\tilde{\beta}_i$  ( $i=1$  to  $N$ ) in Eqs. (11) and (13), we shall adopt a rather elaborate procedure, which will be discussed in great length in Sec. III.

If we now substitute Eq. (6) into Eq. (15) and carry out the variation of the function  $F(\vec{r})$  and the amplitudes  $\tilde{A}_{li}$ , then we obtain the following set of coupled equations:

$$\begin{aligned} \langle \phi_\alpha \phi_d \xi | H - E' | \Psi_0 \rangle_{\vec{r}} \\ + \sum_{i=1}^N \sum_{l=0}^{\infty} \tilde{A}_{li} \langle \phi_\alpha \phi_d \xi | H - E' | \tilde{\chi}_{li} \rangle_{\vec{r}} = 0, \end{aligned} \quad (19a)$$

$$\langle \chi_{lj} | H - E' | \Psi_0 \rangle + \sum_{i=1}^N \tilde{A}_{li} \langle \chi_{lj} | H - E' | \tilde{\chi}_{li} \rangle = 0, \quad (19b)$$

where the subscripts  $l$  and  $j$  in Eq. (19b) take on integral values from 0 to  $\infty$  and from 1 to  $N$ , respectively. Also, in the above equations,  $\Psi_0$  is given by the first term in Eq. (6), and  $\chi_{li}$  and  $\tilde{\chi}_{li}$  are defined as

$$\chi_{li} = \phi_\alpha \phi_i \frac{1}{r} g_{li}(r) P_l(\cos\theta) \xi(s, t), \quad (20)$$

and

$$\tilde{\chi}_{li} = \mathcal{G} \chi_{li}. \quad (21)$$

Further, to simplify writing, we have used the notation  $\langle \rangle_{\vec{r}}$  to indicate integration over internal spatial coordinates of the clusters, summation over spin and isospin coordinates, but no integration over the relative coordinates  $\vec{r}$ .

To demonstrate in a particularly transparent manner how the inclusion of the specific distortion effect influences the result, we shall first consider Eq. (19) in the case where the number of distortion functions is equal to 1. Afterwards, we shall then discuss the way to generalize to the case where many distortion functions are included.

With  $N=1$ , we can solve Eq. (19b) to express

$\tilde{A}_{i1}$  explicitly in terms of  $\Psi_0$ , i.e.,

$$\tilde{A}_{i1} = -\frac{\langle \chi_{i1} | H - E' | \Psi_0 \rangle}{\eta_{i1}(E_{i1} - E')}, \quad (22)$$

where

$$E_{i1} = \frac{\langle \chi_{i1} | H | \tilde{\chi}_{i1} \rangle}{\eta_{i1}}, \quad (23)$$

with

$$\eta_{i1} = \langle \chi_{i1} | \tilde{\chi}_{i1} \rangle. \quad (24)$$

Substitution of Eq. (22) into Eq. (19a) yields (for  $N=1$ )

$$\begin{aligned} \langle \phi_\alpha \phi_d \xi | H - E' | \Psi_0 \rangle_{\vec{r}} \\ = \sum_{i=0}^{\infty} \frac{\langle \phi_\alpha \phi_d \xi | H - E' | \tilde{\chi}_{i1} \rangle_{\vec{r}} \langle \chi_{i1} | H - E' | \Psi_0 \rangle}{\eta_{i1}(E_{i1} - E')}. \end{aligned} \quad (25)$$

The left-hand side of Eq. (25) has been evaluated in our previous study<sup>10</sup> of  $d + \alpha$  scattering, where

as

$$\begin{aligned} \langle \phi_\alpha \phi_d \xi | H - E' | \Psi_0 \rangle_{\vec{r}} = \eta_0 \sum_i \frac{1}{r} P_i(\cos \theta) \\ \times \left\{ \left[ -\frac{\hbar^2}{2\mu} \left( \frac{d^2}{dr^2} - \frac{l(l+1)}{r^2} \right) - E + V_D(r) + V_C(r) \right] f_i(r) + \int_0^\infty \bar{k}_i(r, r') f_i(r') dr' \right\}. \end{aligned} \quad (30)$$

The expressions for the direct nuclear potential  $V_D(r)$ , the direct Coulomb potential  $V_C(r)$ , and the partial-wave kernel function  $k_i(r, r')$  have been given in our previous publication,<sup>10</sup> but they were in a form which is not convenient for our present calculation; hence, for the sake of clarity, they are further given in a more suitable form in Appendix A.

Because of the similarity in the mathematical structure of  $\tilde{\chi}_{i1}$  and  $\Psi_0$ , the right-hand side of Eq. (25) can also be evaluated in a straightforward manner. Thus, it can be easily shown that

$$\langle \phi_\alpha \phi_d \xi | H - E' | \tilde{\chi}_{i1} \rangle_{\vec{r}} = \frac{1}{r} u_{i1}(r) P_l(\cos \theta), \quad (31)$$

where only one  $l$  value contributes. The expression for  $u_{i1}(r)$  is quite lengthy and will be given in Appendix B. Similarly, the quantity  $\langle \chi_{i1} | H - E' | \Psi_0 \rangle$  can be calculated easily; it is

$$\langle \chi_{i1} | H - E' | \Psi_0 \rangle = \frac{4\pi}{2l+1} \int_0^\infty f_i(r') u_{i1}^*(r') dr'. \quad (32)$$

Finally, by combining Eqs. (25), (30)–(32), we

it was shown that

$$\begin{aligned} \langle \phi_\alpha \phi_d \xi | H - E' | \Psi_0 \rangle_{\vec{r}} \\ = \eta_0 \left\{ \left[ -\frac{\hbar^2}{2\mu} \nabla^2 - E + V_D(r) + V_C(r) \right] F(\vec{r}) \right. \\ \left. + \int K(\vec{r}, \vec{r}') F(\vec{r}') d\vec{r}' \right\}, \end{aligned} \quad (26)$$

with  $E$  being the c.m. relative energy of the deuteron and the  $\alpha$  clusters,  $\mu$  being the reduced mass of the system, and  $\eta_0$  defined by the equation

$$\eta_0 = \langle \phi_\alpha \phi_d \xi | \phi_\alpha \phi_d \xi \rangle_{\vec{r}}. \quad (27)$$

If we now make the expansion

$$F(\vec{r}) = \sum_i \frac{1}{r} f_i(r) P_l(\cos \theta) \quad (28)$$

and

$$K(\vec{r}, \vec{r}') = \frac{1}{4\pi r r'} \sum_l (2l+1) k_l(r, r') P_l(\nu), \quad (29)$$

with  $\nu = \vec{r} \cdot \vec{r}' / r r'$ , then Eq. (26) can be rewritten

obtain the following equation which  $f_i$  satisfies:

$$\begin{aligned} \left[ \frac{\hbar^2}{2\mu} \left( \frac{d^2}{dr^2} - \frac{l(l+1)}{r^2} \right) + E - V_D(r) - V_C(r) \right] f_i(r) \\ = \int_0^\infty [k_i(r, r') + \bar{k}_{i1}(r, r')] f_i(r') dr', \end{aligned} \quad (33)$$

with

$$\bar{k}_{i1}(r, r') = \frac{4\pi}{2l+1} \frac{1}{\eta_0 \eta_{i1}} \frac{1}{E' - E_{i1}} u_{i1}(r) u_{i1}^*(r'). \quad (34)$$

As is seen, Eq. (33) is the usual no-distortion resonating-group equation augmented by an additional nonlocal interaction, characterized by a separable kernel function  $\bar{k}_{i1}(r, r')$ . This kernel function  $\bar{k}_{i1}$  therefore represents the effect of the coupling of the distortion function  $\tilde{\chi}_{i1}$  with the function  $\Psi_0$ , i.e., the deuteron specific distortion effect.

It is a rather simple procedure to generalize to the case where  $N$  distortion functions are

added to  $\Psi_0$ . The only complication arises because the functions  $\tilde{\chi}_{li}$  are not orthogonal to each other. This means that Eq. (19b) describes a coupled system which must be solved for  $\tilde{A}_{li}$ . This complication can be overcome by transforming to a basis set of functions  $\tilde{\psi}_{li}$  which are linear combinations of  $\tilde{\chi}_{li}$ , but have the following properties:

$$\langle \psi_{l'j} | \tilde{\psi}_{li} \rangle = \delta_{l'l} \delta_{ij} \quad (35a)$$

and

$$\langle \psi_{l'j} | H | \tilde{\psi}_{li} \rangle = E_{li} \delta_{l'l} \delta_{ij}, \quad (35b)$$

where  $\psi_{l'j}$  denotes the unantisymmetrized part of  $\tilde{\psi}_{l'j}$  [see Eq. (21)]. With this new set of functions, the trial function  $\Psi_N$  then has the form

$$\Psi_N = \Psi_0 + \sum_{i=1}^N \sum_{l=0}^{\infty} \tilde{B}_{li} \tilde{\psi}_{li}, \quad (36)$$

and we can proceed in a similar way as in the one-distortion-function case. The result is

$$\begin{aligned} & \langle \phi_\alpha \phi_d \xi | H - E' | \Psi_0 \rangle_{\vec{r}} \\ &= \sum_{i=1}^N \sum_{l=0}^{\infty} \frac{\langle \phi_\alpha \phi_d \xi | H - E' | \tilde{\psi}_{li} \rangle_{\vec{r}} \langle \psi_{li} | H - E' | \Psi_0 \rangle}{E_{li} - E'}. \end{aligned} \quad (37)$$

Equation (37) is quite similar to Eq. (25), except for the fact that there are now  $N$  separable kernel functions, corresponding to the adoption of  $N$  distortion functions  $\tilde{\psi}_{li}$ . Also, we should point out here that, since separable kernel functions are involved, one can obtain a formal solution of Eq. (37) for  $\Psi_0$  by using the Green-function technique. From this solution, one can then compute the scattering amplitude which exhibits the familiar Breit-Wigner  $N$ -level resonance structure.<sup>11, 12</sup>

One can also see from the structure of Eq. (37) how the inclusion of the distortion functions  $\tilde{\psi}_{li}$  modifies the form of the equation [Eq. (2)] in the no-distortion approximation. As is easily seen, Eq. (37) can be written in the form

$$\langle \phi_\alpha \phi_d \xi | H + \tilde{V} - E' | \Psi_0 \rangle_{\vec{r}} = 0, \quad (38)$$

with

$$\tilde{V} = \sum_{i=1}^N \sum_{l=0}^{\infty} \frac{(H - E') | \tilde{\psi}_{li} \rangle \langle \psi_{li} | (H - E')}{E' - E_{li}}. \quad (39)$$

Thus, the consideration of the deuteron specific distortion effect, through the use of distortion functions, introduces into the formulation an additional nonlocal energy-dependent interaction, which describes the coupling of the compound-nucleus states  $\tilde{\psi}_{li}$  to the elastic scattering state  $\Psi_0$ . In what follows, we shall compare the solu-

tion of Eq. (2) with that of Eq. (38) in order to determine the importance of  $\tilde{V}$  in the  $d+\alpha$  problem. Before this comparison can be made, however, we must first discuss a way to determine the nonlinear parameters  $\tilde{\alpha}_i$  and  $\tilde{\beta}_i$  contained in the distortion functions. This discussion is given in the next section.

### III. CHOICE OF NONLINEAR PARAMETERS IN THE DISTORTION FUNCTIONS

Our first task is to determine the values of the parameters  $\tilde{\alpha}_i$  and  $\tilde{\beta}_i$  in the distortion functions. In principle, this can be achieved by searching for a minimum value of the expectation value of the Hamiltonian  $H$  in the bound-state case, or a stationary behavior of the phase shift in the scattering case. However, because of the nonlinear nature of these parameters, this procedure will be feasible only when the number of distortion functions is rather small, i.e.,  $N=1$  or at most 2 in Eq. (6). Hence, we have adopted a more practical method in this calculation. This method consists in the selection of a suitable set of  $(\tilde{\alpha}_i, \tilde{\beta}_i)$  values to be used at all values of relative energy  $E$  and orbital angular momentum  $l$  under consideration. The relative lack of freedom in such a choice of no energy and  $l$  dependence for these parameters is then compensated for by the adoption of a large number of distortion functions. In this way, there are only linear variational parameters  $\tilde{A}_{li}$  and the linear variational function  $F(\vec{r})$  involved, and these can be easily determined by the usual numerical techniques.

To obtain a guide about how to select an appropriate set of  $(\tilde{\alpha}_i, \tilde{\beta}_i)$  values in the many distortion-function case, we consider in great detail the  $l=0$ , bound-state problem with a single distortion function and  $u=0.95$ .<sup>13</sup> In this particular case, our procedure is to find, for every choice

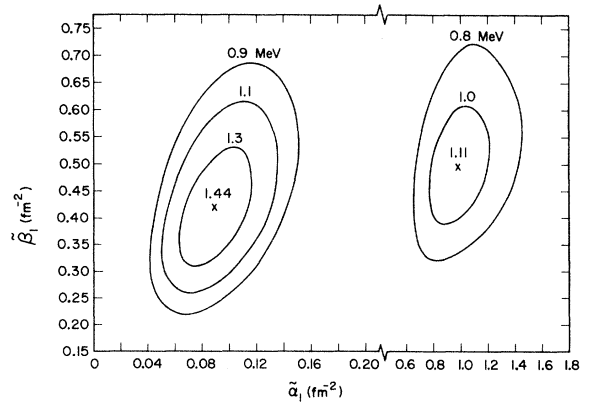


FIG. 1. Contour plot of the  $d+\alpha$  separation energy  $E_B$  in the  $(\tilde{\alpha}_1, \tilde{\beta}_1)$  parameter space.

TABLE I. Values of parameters  $\tilde{\alpha}_i$  and  $\tilde{\beta}_i$ , in  $\text{fm}^{-2}$ , in various distortion-function configurations.

Index $i$	Distortion-function configuration									
	I		II		III		IV		V	
	$\tilde{\alpha}_i$	$\tilde{\beta}_i$	$\tilde{\alpha}_i$	$\tilde{\beta}_i$	$\tilde{\alpha}_i$	$\tilde{\beta}_i$	$\tilde{\alpha}_i$	$\tilde{\beta}_i$	$\tilde{\alpha}_i$	$\tilde{\beta}_i$
1	0.07	0.45	0.07	0.49	0.10	0.45	0.09	0.41	1.00	0.50
2	1.20	0.45	0.25	0.49	1.00	0.53	0.09	0.60	1.00	0.68
3	0.25	0.45	0.60	0.49	0.50	0.49	0.09	0.23	1.00	0.30
4	0.07	0.27	0.07	0.30	0.20	0.34	0.07	0.41	0.70	0.50
5	1.20	0.27	0.25	0.30	0.90	0.38	0.25	0.41	1.20	0.50
6	0.25	0.27	0.60	0.30	0.25	0.56				
7	0.07	0.63	0.07	0.68	0.55	0.36				
8	1.20	0.63	0.25	0.68	0.70	0.54				
9	0.25	0.63	0.60	0.68	0.95	0.60				

of  $\tilde{\alpha}_1$  and  $\tilde{\beta}_1$  in the distortion function  $\tilde{\chi}_{01}$ , the value of  $E$  for which Eq. (33) has a solution with the appropriate asymptotic behavior. This value is then the negative of the  $\alpha+d$  separation or binding energy  $E_B$  in the ground state of  ${}^6\text{Li}$ . In Fig. 1, we show contours of  $E_B$  in the  $(\tilde{\alpha}_1, \tilde{\beta}_1)$  parameter space. It is interesting to note that there are two local maxima at  $(\tilde{\alpha}_1, \tilde{\beta}_1)$  values of  $(0.089, 0.42 \text{ fm}^{-2})$  and  $(0.98, 0.49 \text{ fm}^{-2})$ . The values of  $\tilde{\alpha}_1$  at these maxima yield deuteron rms radii of 2.91 and 0.88 fm, which are, respectively, larger and smaller than the free deuteron rms radius of about 1.95 fm.

The values of  $E_B$  at the two local maxima are equal to 1.44 and 1.11 MeV, respectively. These should be compared with the result from the no-distortion ( $N=0$ ) case, in which the deuteron and the  $\alpha$  clusters are not even bound, but form a  $l=0$  resonance state at 0.25 MeV. Thus, already from a simple one-distortion-function calculation, we see that the specific distortion of the deuteron has a significant effect. This was also the conclusion reached by Jacobs, Wildermuth, and Wurster.<sup>8</sup>

If the function  $\tilde{\chi}_{01}$  alone is used to describe the ground state of  ${}^6\text{Li}$ , then the optimum values of  $(\tilde{\alpha}_1, \tilde{\beta}_1)$  turn out to be equal to  $(0.64, 0.24 \text{ fm}^{-2})$ . These values are appreciably different from those found at the two local maxima shown in Fig. 1. This means that  $\tilde{\chi}_{01}$  by itself does not give an adequate description of the ground-state behavior in  ${}^6\text{Li}$ , and  $\Psi_0$  is also needed.

Next, we proceed to the case where more than one distortion function is used. As mentioned above, it is now impractical to vary all the nonlinear parameters, so what we do is to use the contour plot of Fig. 1 to make a judicious choice of values for the nonlinear parameters in the many distortion functions; that is, we choose a set of  $(\tilde{\alpha}_i, \tilde{\beta}_i)$  values such that regions near the one-distortion-function maxima are well represented. To make certain that the resultant choice is in fact appropriate, we have examined a large num-

TABLE II. Variation of  $E_B$  with various distortion-function configurations.

Distortion-function configuration	$E_B$ (MeV)
I	1.78
II	1.73
III	1.63
IV	1.55
V	1.49

ber of  $(\tilde{\alpha}_i, \tilde{\beta}_i)$  sets or configurations. In Table I we summarize some of these configurations, while in Table II we list the corresponding values of  $E_B$  in the  $l=0$  ground state. Configuration V is chosen to favor the one-distortion-function maximum at  $(0.98, 0.49 \text{ fm}^{-2})$ , while configuration IV is chosen to favor the one-distortion-function maximum at  $(0.089, 0.42 \text{ fm}^{-2})$ . Configurations I, II, and III involve different nine distortion functions and are chosen to encompass both of these maxima. One can see from Table II that the values of  $E_B$  obtained with nine distortion functions are quite similar and are all greatly improved over the result of the no-distortion calculation. In fact, even the choice of configurations IV and V with five distortion functions seems to yield reasonable results. Thus, it is our opinion that

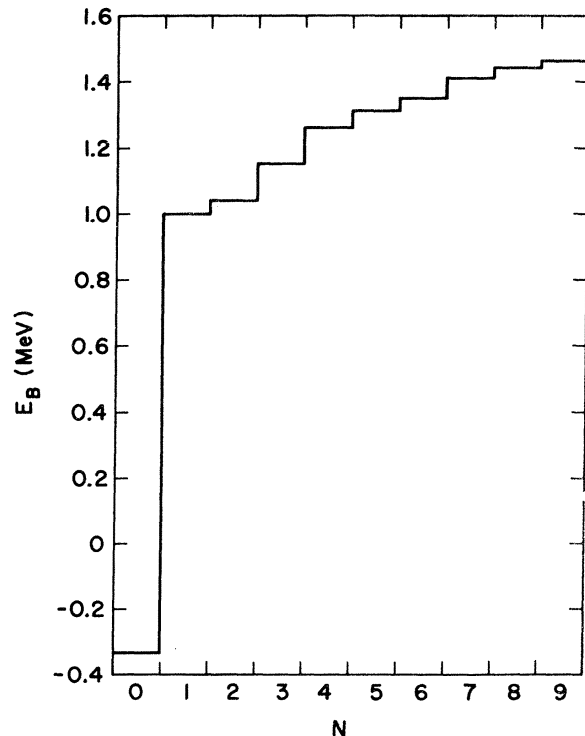


FIG. 2.  $d+\alpha$  separation energy  $E_B$  as a function of the number of distortion functions.

with configuration I in particular, our calculation will contain the freedom necessary to describe adequately the deuteron specific distortion effect, and any addition to this configuration will only affect the value of  $E_B$  to a rather insignificant extent.

The above-mentioned convergence is further illustrated in Fig. 2, where the value of  $E_B$  is shown as a function of the number of distortion functions in configuration I. To obtain this figure, the value of the exchange-mixture parameter  $u$  is set as 0.925, so that the value of  $E_B$  for  $N=9$  is equal to the experimentally determined value of 1.47 MeV.<sup>10</sup> From this figure, we see that the  $E_B$  values for  $N=0, 3, 6,$  and  $9$  are equal to  $-0.34, 1.16, 1.36,$  and  $1.47$  MeV, respectively, which does indicate that with the choice of configuration I, the addition of more distortion functions is unlikely to make any significant improvement in the ground-state separation energy of  ${}^6\text{Li}$ .

Phase shifts for  $l=0, 1, 2,$  and  $3$  over a wide range of energies have also been examined using various distortion configurations, and a similar convergence feature as that discussed above has also been observed. This is shown in Fig. 3, where we depict the  $l=0$  and  $2$  phase shifts calculated with  $N=0, 3,$  and  $9$  in configuration I and  $u=0.925$ . Phase shifts for  $l=1$  and  $3$  as a function of  $N$  are not shown, since, as will be discussed in the next section, specific distortion effect has only minor influence on these phase shifts. As is seen, the difference in the results for  $N=3$  and  $9$  is much smaller than that for  $N=0$  and  $3$ , indicating therefore that the choice of configuration I is also appropriate for a study of the  $d + \alpha$  problem in the positive-energy ( $E > 0$ ) region.

Even though in our distortion functions, the width parameter  $\alpha$  of the  $\alpha$  cluster is fixed at  $0.514 \text{ fm}^{-2}$ , it is still necessary to make certain that the freedom in the distortion functions is not being used to improve the internal energy of this cluster. For this purpose, we have also made a study, similar to that described above, with  $\alpha = 0.80 \text{ fm}^{-2}$ , a value which optimizes the expectation value of the  $\alpha$ -particle Hamiltonian with the wave function  $\phi_\alpha$  of Eq. (7). The result shows that the convergence properties exhibited by  $E_B$  as a function of  $N$  are very similar to those discussed above with  $\alpha = 0.514 \text{ fm}^{-2}$ .<sup>14</sup> This means therefore that the addition of the distortion functions of Eq. (6) does indeed correct for the deuteron specific distortion effect, rather than causes a collapse of the  $\alpha$  cluster.

Recently, an investigation by Schwager and Schmid<sup>15</sup> has shown that, in the fictitious case of the elastic scattering of a boson by a bound boson pair, the phase shift shows a nonconvergent be-

havior when an approximate wave function is used to describe the boson pair. In our case, such a nonconvergent behavior does not appear even when nine distortion functions are used, since the deuteron function  $\phi_d$  used here is a very good representation of the spatial part of the deuteron eigenfunction.<sup>6</sup>

In conclusion, then, we find that the deuteron specific distortion effect can be examined at all energy and orbital angular momentum values by simply varying the linear parameters  $\tilde{A}_{1i}$  in the distortion functions of configuration I. This configuration, together with  $u=0.925$ , will therefore be employed in all subsequent calculations to be discussed in the following sections.

#### IV. RESULTS AND DISCUSSION

##### A. Phase Shifts and Differential Cross Sections

As was mentioned in the previous section, the exchange-mixture parameter  $u$  in our nucleon-nucleon potential of Eq. (4) is adjusted such that the solution of Eq. (37) with the nine distortion functions of configuration I yields the experimental  $d + \alpha$  separation energy of 1.47 MeV. The resultant value for  $u$  is 0.925, which is much smaller than the value of 1.175 required in the no-distortion approximation. Thus, from this calculation alone, we can already see that the specific distortion of the deuteron cluster has a significant effect and should certainly be properly considered in the  $d + \alpha$  problem.

The finding of  $u=0.925$  is indeed quite gratifying. In the no-distortion calculation of  $\alpha + \alpha$  scattering,<sup>4</sup> where the specific distortion effect is relatively minor,<sup>7</sup> it has been found that a choice of  $u=0.92$  yielded an over-all good agreement with the empirical  $\alpha + \alpha$  phase shifts over a wide energy range. Therefore, with the specific distortion effect taken into account in the  $d + \alpha$  calculation through the addition of the functions  $\tilde{\chi}_{1i}$  or  $\tilde{\psi}_{1i}$ , we do obtain a consistent treatment, in the sense that we can now use the same nucleon-nucleon potential to describe the behavior of both the  $\alpha + \alpha$  and the  $d + \alpha$  systems.

In Figs. 4 and 5, we show the effect of including the distortion functions on the even- $l$  and odd- $l$  phase shifts for energies in the range of 0–28 MeV.<sup>16</sup> In these figures, the solid curves represent the results of the calculation with distortion functions, while the dashed curves show the no-distortion results. The data points represent the real parts of the empirical phase shifts determined by McIntyre and Haerberli<sup>17</sup> in the energy region from 1.3 to 6.7 MeV and by Darriulat *et al.*<sup>18</sup> in the energy region from 6.7 to 18.2 MeV. The  $l=4, 5,$  and  $6$  phase shifts are rather small in the energy range considered here and specific

distortion effects have not been included in their computation; hence, only dashed curves are shown for these phase shifts in these two figures.

The salient features contained in Figs. 4 and 5 are as follows:

- (i) Specific distortion effects are important in the even- $l$  cases, but much less so in the odd- $l$  cases.
- (ii) Phase shifts calculated in the no-distortion approximation are consistently smaller than those calculated with distortion functions. In particular, it is noted that in the  $l=0$ , no-distortion case, the phase-shift behavior indicates the nonexistence of a bound  $d+\alpha$  system, but only the appearance of a resonance structure at about 0.34 MeV.
- (iii) In the  $l=0$  case, the phase shifts calculated with distortion functions agree quite well with the empirical phases over the entire energy range considered. For the other phase shifts, the lack of a noncentral component in our nucleon-nucleon potential and consequently, the lack of splitting of the phases does not really allow a detailed comparison with the empirical phases to be made; however, we can still see from Figs. 4 and 5 that, in general, the agreement is rather satisfactory.

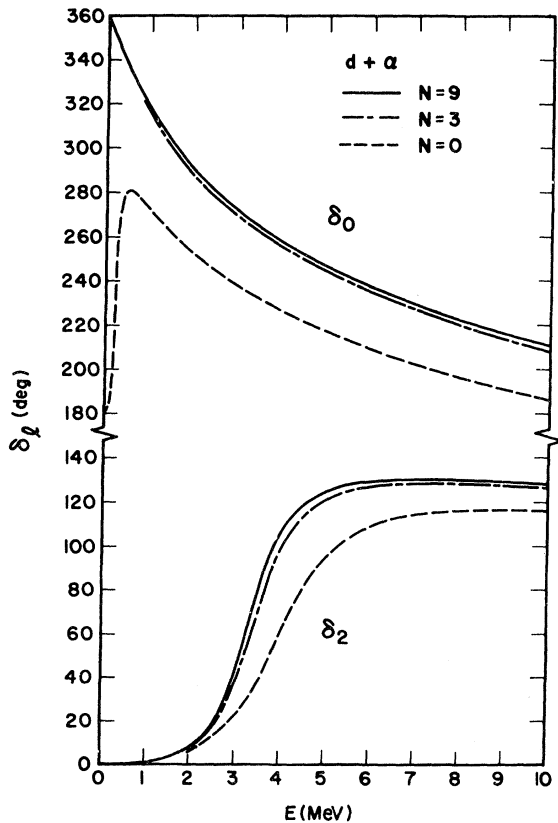


FIG. 3. Even- $l$  phase shifts  $\delta_0$  and  $\delta_2$  as a function of  $E$  with different number of distortion functions.

- (iv) There are sharp resonance structures at energies above 12 MeV in the phase shifts calculated with distortion functions. This will be discussed in detail in Sec. IV B.

The occurrence of the odd-even behavior as mentioned in (i) above is really not surprising. In a calculation where a totally antisymmetrized wave function is employed, odd-even features do occur rather frequently. For example, it occurs even in the phase-shift values at a fixed energy, as is depicted in Fig. 6. In this figure, we show  $\delta_l$  as a function of  $l$  at 15 MeV for both the  $d+\alpha$  and the  ${}^3\text{He}+\alpha$  systems. Here it can be seen that the odd-even behavior is not only quite apparent, but is also rather different in these two systems.

To obtain a quantitative estimate of the specific distortion effect, we have determined the values of  $u$  in the no-distortion case, to be called  $u_l^{\text{eff}}(E)$ ,

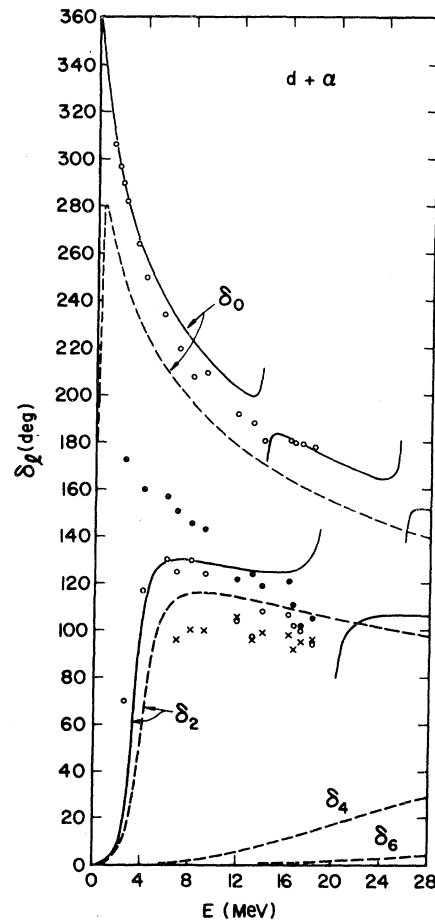


FIG. 4. Even- $l$  phase shifts in the energy range 0-28 MeV. The solid curves represent the results of the calculation with the nine distortion functions of configuration I, while the dashed curves show the no-distortion results. Experimental data points are those of Refs. 17 and 18.



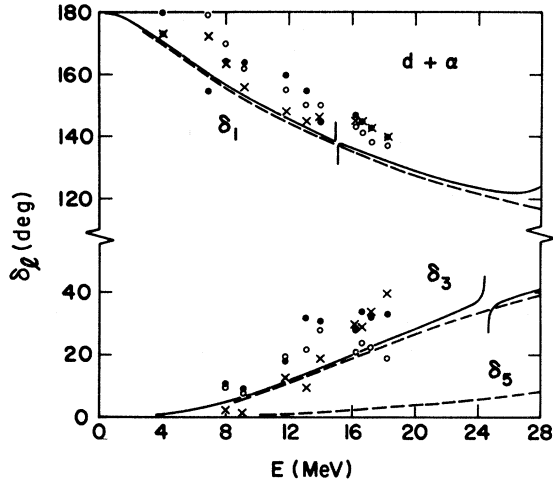


FIG. 5. Odd- $l$  phase shifts in the energy range 0–28 MeV. The solid curves represent the results of the calculation with the nine distortion functions of configuration I, while the dashed curves show the no-distortion results. Experimental data points are those of Refs. 17 and 18.

which are necessary to achieve an agreement with the phase-shift results of the calculation with distortion functions. In Table III, we list the values of  $u_l^c$ , defined as

$$u_l^c(E) = u_l^{\text{eff}}(E) - 0.925 \quad (40)$$

in the  $l=0$  case. Here it is seen that the values of  $u_0^c$  decrease quite rapidly with energy, which is a confirmation of one's intuitive feeling that specific

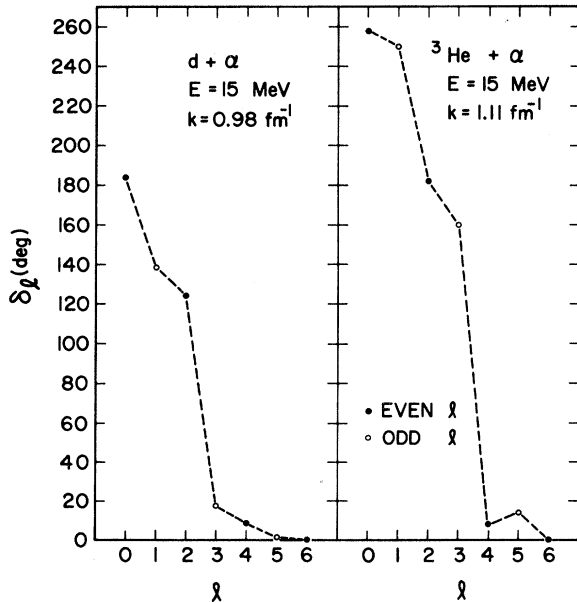


FIG. 6. Odd-even behavior of the phase shifts at 15 MeV in the  $d + \alpha$  and  ${}^3\text{He} + \alpha$  systems.

distortion effects should become less important at higher energies. Similar determinations have also been made for  $u_l^c$  with  $l \neq 0$ . For  $l=1$  and 3, the values of  $u_l^c$  are rather small, being only about 0.02 in the energy region less than about 20 MeV. In the case of  $l=2$ , the values of  $u_l^c$  are equal to about 0.1 in the low-energy region, but again become smaller as the energy increases.

The decrease in  $u_l^c$  with energy indicates to us that at a sufficiently high energy, one should be able to omit the specific distortion effect entirely. To see if this is indeed so, we have made a no-distortion calculation of  $d + \alpha$  scattering at 55 MeV with  $u = 0.925$ . The fact that at this energy, many reaction channels are open is taken into account crudely by introducing into the no-distortion formulation a phenomenological imaginary potential  $iW(r)$ , with

$$W(r) = -W_0 \left\{ \frac{1}{1 + e^{(r-R)/a}} + \frac{4e^{(r-R)/a}}{[1 + e^{(r-R)/a}]^2} \right\} \quad (41)$$

and  $R=3.3$  fm,  $a=0.5$  fm. The quantity  $W_0$  is then adjusted to yield a best agreement with the experimental data at 55 MeV of Tatischeff and Brissand.<sup>20</sup> The resultant differential cross section obtained with  $W_0=2$  MeV, which results in a total reaction cross section of 269 mb, is shown in Fig. 7, while the corresponding complex phase shifts are given in Table IV. From Fig. 7, it can be seen that the agreement between calculated and experimental results is quite satisfactory, thus further supporting the assertion that the specific distortion effect is not important at higher energies.

#### B. Compound-Nucleus Resonances

We now turn our attention to the compound-nucleus resonances which are clearly seen in the phase-shift graphs of Figs. 4 and 5. These resonances are plotted as breaks in the curves for convenience, but they do exhibit the usual resonance structure.

The existence of compound-nucleus resonances is expected in our calculation, since it is well known<sup>11,12</sup> that the coupling of an open channel to

TABLE III.  $u_l^c$  as a function of  $E$ .

$E$ (MeV)	$u_l^c$
4	0.22
8	0.20
12	0.19
16	0.16
22	0.14
32	0.09

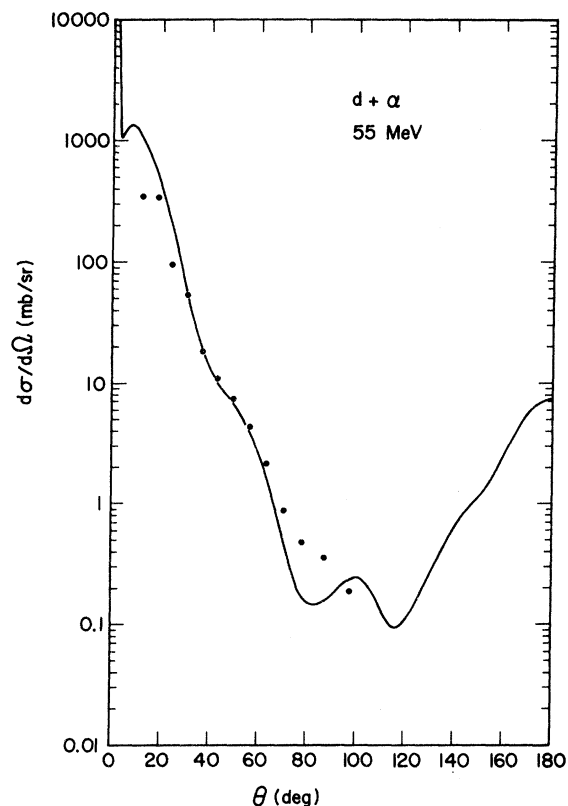


FIG. 7. Comparison of calculated differential cross section at 55 MeV with the experimental data of Ref. 20.

a bound-state function will give rise to a scattering amplitude which has the Breit-Wigner resonance form. We can in fact make a one-to-one correspondence of the characteristic energies  $\tilde{E}_{ii}$  of configuration I to the calculated resonance energies in the various partial waves. These characteristic energies, defined as

$$\tilde{E}_{ii} = E_{ii} - E_{\alpha} - E_d, \quad (42)$$

where  $E_{ii}$  is given by Eq. (35b), and  $E_{\alpha}$  and  $E_d$

TABLE IV.  $d + \alpha$  phase shifts at 55 MeV.

$l$	$\delta_l$ (deg)
0	97.10 + $i$ 11.57
1	79.66 + $i$ 13.15
2	78.08 + $i$ 8.67
3	51.49 + $i$ 10.54
4	43.71 + $i$ 9.77
5	21.40 + $i$ 10.53
6	14.14 + $i$ 7.07
7	6.62 + $i$ 3.72
8	3.84 + $i$ 1.70
9	1.87 + $i$ 0.70
10	1.00 + $i$ 0.28
11	0.50 + $i$ 0.11

are the expectation values of the  $\alpha$  and deuteron Hamiltonians computed with the wave functions of Eqs. (7) and (9), are listed in Table V. They represent of course our variational estimate, using the basis functions  $\tilde{\psi}_{ii}$ , of the  $T=0$  level structure of  ${}^6\text{Li}$  in the absence of any open channels. With the inclusion of the  $d + \alpha$  scattering channel, the compound system will be able to decay and each of the compound-nucleus levels will acquire a finite width and shift its position in energy. For example, the level parameters for the  $l=0$  level at 14.05 MeV and the  $l=2$  level at 19.57 MeV (See Fig. 4) can be obtained by examining the calculated results and these parameters are given in Table VI.

It should be emphasized that the positions and widths of the compound-nucleus resonance levels are determined under our model assumption that there is only one open channel, namely, the  $d + \alpha$  channel, in our calculation. One must be aware of the fact that if more open channels, such as the  ${}^3\text{He} + {}^3\text{H}$  and the  $\alpha + n + p$  channels, are introduced into our formulation, these positions and widths may appreciably change. In fact, it is quite likely that with the consideration of these additional open channels, some of the levels may disappear entirely from the calculation. Therefore, we feel that, until a better calculation involving more open channels is made, it may be advisable not to take them seriously at this present moment.

On the other hand, there is some experimental evidence which suggests that at energies above 12 MeV, compound-nucleus resonances may contribute significantly to the  $d + \alpha$  differential cross sections. An inspection of Fig. 2 in the paper by Darrulat *et al.*<sup>18</sup> shows that the experimental differential cross section begins to change its shape quite drastically at about 12 MeV, in distinct contrast with our finding<sup>10</sup> in the no-distortion approximation that the shapes of the differential cross-section curves at 5.98 to 16.58 MeV remain about the same.

TABLE V. Characteristic energies  $\tilde{E}_{ii}$  of distortion-function configuration I.

Index $i$	$\tilde{E}_{0i}$ (MeV)	$\tilde{E}_{1i}$ (MeV)	$\tilde{E}_{2i}$ (MeV)	$\tilde{E}_{3i}$ (MeV)
1	0.69	11.51	4.93	17.76
2	14.89	15.34	19.24	24.55
3	21.20	30.34	24.69	40.41
4	27.35	37.76	42.28	51.43
5	47.74	38.83	44.76	52.28
6	51.03	56.24	62.39	75.37
7	64.35	59.29	66.52	84.07
8	76.22	82.18	91.03	104.45
9	118.94	101.81	106.76	121.45

TABLE VI. Resonance energies and level parameters for two compound-nucleus levels.

	Level 1	Level 2
$l$	0	2
Characteristic energy (MeV)	14.89	19.24
Resonance energy (MeV)	14.05	19.57
Level shift (MeV)	0.84	-0.33
Level width (MeV)	0.15	0.80

### V. CONCLUSION

In this investigation, we have examined the effect of deuteron specific distortion in the  $d + \alpha$  problem by means of a microscopic procedure. This procedure consists in the addition of a large number of square-integrable or distortion functions with linear variational amplitudes into the usual no-distortion resonating-group wave function. The result shows that this effect is indeed quite important and its consideration leads to the consequence that the same nucleon-nucleon potential can now be used to yield a consistent and satisfactory treatment in both the  $\alpha + \alpha$  and  $d + \alpha$  systems.

The specific distortion effect in the  $d + \alpha$  case is shown to be quite important in even- $l$  states, but not in odd- $l$  states. In the  $l=0$  state, for instance, its inclusion increases the phase-shift

value by more than  $20^\circ$  in the low-energy region. As the energy increases, this effect does become less important, in agreement with one's intuitive feeling. At 55 MeV, for example, it is found that even a total omission of this effect does not cause any serious compromise in fit with the experimental data.

The addition of distortion functions also causes the appearance of resonance structures in the various partial-wave scattering amplitudes. These resonances arise of course from the coupling of the compound-nucleus states with the elastic scattering channel. Since at the energies where they occur, there are several reaction channels open, it is quite possible that our model assumption of a single open  $d + \alpha$  channel in the calculation may create an unrealistic determination of the widths and positions of these resonances. In view of this, we feel that in order to obtain more reliable information about these resonance levels, it may be necessary to perform a better calculation, which involves all the important reaction channels, in particular, the three-body-breakup  $\alpha + n + p$  channel.

In conclusion, we feel that our calculation has demonstrated the importance of the specific distortion effect, and consequently, a proper consideration of this effect should be included in all calculations where a deuteron cluster, or even a  $^3\text{H}$  or  $^3\text{He}$  cluster, is involved.

### APPENDIX A: EXPRESSIONS FOR $V_D(r)$ , $V_C(r)$ , AND $k_l(r, r')$

The expressions for the quantities  $V_D(r)$ ,  $V_C(r)$ , and  $k_l(r, r')$  were given in Ref. 10. These expressions were, however, explicitly calculated for the case with a two-Gaussian deuteron function and a simpler nucleon-nucleon potential, and were in a form which is not convenient for our calculation with distortion functions. Hence, for the sake of clarity, they are also given here for our present case with the deuteron function of Eqs. (9) and (10) and the nucleon-nucleon potential of Eqs. (4), (17), and (18), and in a form which is much more suitable for our present purposes.

The direct nuclear potential  $V_D(r)$  is given by

$$V_D(r) = -\frac{1}{G_0} \sum_{k=1}^2 V_{0k} w_{15}^0 \sum_{p=1}^3 \sum_{q=1}^3 A_p A_q \left( \frac{\pi^3}{4\alpha^3} \right)^{3/2} \left( \frac{\pi}{\alpha_p + \alpha_q} \right)^{3/2} \left[ \frac{4\alpha(\alpha_p + \alpha_q)}{4\alpha(\alpha_p + \alpha_q) + \kappa_k(4\alpha + 3\alpha_p + 3\alpha_q)} \right]^{3/2} \times \exp \left[ -\frac{4\alpha(\alpha_p + \alpha_q)\kappa_k}{4\alpha(\alpha_p + \alpha_q) + \kappa_k(4\alpha + 3\alpha_p + 3\alpha_q)} r^2 \right], \quad (\text{A1})$$

with

$$G_0 = \sum_{p=1}^3 \sum_{q=1}^3 A_p A_q \left( \frac{\pi^3}{4\alpha^3} \right)^{3/2} \left( \frac{\pi}{\alpha_p + \alpha_q} \right)^{3/2}. \quad (\text{A2})$$

In the above expressions,

$$V_{01} = V_{0t}, \quad V_{02} = V_{0s}, \quad \kappa_1 = \kappa_t, \quad \kappa_2 = \kappa_s, \quad (\text{A3})$$

with the numerical values of these quantities given by Eqs. (17) and (18), while  $A_p$  and  $\alpha_p$  are given by Eq. (10). Also, we have defined

$$w_{15}^0 = 8w_k - 2m_k + 4b_k - 4h_k, \quad (\text{A4})$$

with

$$w_1 = b_1 = \frac{1}{4}u, \quad m_1 = h_1 = \frac{1}{4}(2-u), \quad w_2 = -b_2 = \frac{1}{4}u, \quad m_2 = -h_2 = \frac{1}{4}(2-u). \quad (\text{A5})$$

The direct Coulomb potential  $V_c(r)$  has the form

$$V_c(r) = \frac{1}{G_0} \frac{zz'e^2}{r} \sum_{p=1}^3 \sum_{q=1}^3 A_p A_q \left( \frac{\pi^3}{4\alpha^3} \right)^{3/2} \left( \frac{\pi}{\alpha_p + \alpha_q} \right)^{3/2} \Phi \left[ \left( \frac{4\alpha(\alpha_p + \alpha_q)}{4\alpha + 3\alpha_p + 3\alpha_q} \right)^{1/2} r \right], \quad (\text{A6})$$

with  $z$  and  $z'$  being the atomic numbers of the  $\alpha$  and the deuteron, respectively, and

$$\Phi(x) = \frac{2}{\sqrt{\pi}} \int_0^x e^{-t^2} dt. \quad (\text{A7})$$

The kernel function  $k_l(r, r')$  is given by

$$k_l(r, r') = \frac{1}{G_0} \sum_{p=1}^3 \sum_{q=1}^3 A_p A_q \left[ -\frac{\hbar^2}{2M} \mathcal{T}_{pq} - \sum_{k=1}^2 V_{0k} \mathfrak{V}_{k,pq} + E' \mathcal{G}_{pq} \right], \quad (\text{A8})$$

where

$$E' = E_\alpha + E_d + E, \quad (\text{A9})$$

with

$$E_\alpha = \frac{\hbar^2}{2M} \frac{9}{2} \alpha - \sum_{k=1}^2 6(w_k + m_k) V_{0k} \left( \frac{\alpha}{\alpha + 2\kappa_k} \right)^{3/2} + \frac{1}{2} z(z-1) e^2 \left( \frac{2\alpha}{\pi} \right)^{1/2} \quad (\text{A10})$$

and

$$E_d = \frac{1}{G_0} \sum_{p=1}^3 \sum_{q=1}^3 A_p A_q \left( \frac{\pi^3}{4\alpha^3} \right)^{3/2} \left( \frac{\pi}{\alpha_p + \alpha_q} \right)^{3/2} \left[ \frac{\hbar^2}{2M} \frac{3\alpha_p \alpha_q}{\alpha_p + \alpha_q} - V_{01} \left( \frac{\alpha_p + \alpha_q}{\alpha_p + \alpha_q + 4\kappa_1} \right)^{3/2} + \frac{1}{2} z'(z'-1) e^2 \left( \frac{\alpha_p + \alpha_q}{\pi} \right)^{1/2} \right]. \quad (\text{A11})$$

The quantities  $\mathcal{T}_{pq}$ ,  $\mathfrak{V}_{k,pq}$ , and  $\mathcal{G}_{pq}$  in Eq. (A8) are defined as follows:

$$\begin{aligned} \mathcal{T}_{pq} = & 2\epsilon_1 \left\{ \left[ \frac{24\alpha^2 + 35\alpha(\alpha_p + \alpha_q) + 15\alpha_p \alpha_q}{4\alpha + 3(\alpha_p + \alpha_q)} - Q_a r^2 - Q_b r'^2 \right] S_l \left( -\frac{2}{3} c_1 \right) + Q_c r r' T_l \left( -\frac{2}{3} c_1 \right) \right\} \exp \left[ -\frac{2}{3} (a_1 r^2 + b_1 r'^2) \right] \\ & - \epsilon_2 \left\{ \left[ \frac{25}{2} \alpha + \frac{3\alpha(\alpha_p \alpha_q - \alpha^2)}{(\alpha + \alpha_p)(\alpha + \alpha_q)} - \frac{112}{27} \alpha^2 (r^2 + r'^2) \right] S_l \left( -\frac{2}{3} c_2 \right) - \frac{208}{27} \alpha^2 r r' T_l \left( -\frac{2}{3} c_2 \right) \right\} \exp \left[ -\frac{2}{3} (a_2 r^2 + b_2 r'^2) \right], \end{aligned} \quad (\text{A12})$$

$$\begin{aligned} \mathfrak{V}_{k,pq} = & -2\epsilon_1 \left\{ w_{23}^1 \epsilon_{23}^1 S_l \left( -\frac{2}{3} c_{23}^1 \right) \exp \left[ -\frac{2}{3} (a_{23}^1 r^2 + b_{23}^1 r'^2) \right] + w_{15}^1 \epsilon_{15}^1 S_l \left( -\frac{2}{3} c_{15}^1 \right) \exp \left[ -\frac{2}{3} (a_{15}^1 r^2 + b_{15}^1 r'^2) \right] \right. \\ & + w_{26}^1 \epsilon_{26}^1 S_l \left( -\frac{2}{3} c_{26}^1 \right) \exp \left[ -\frac{2}{3} (a_{26}^1 r^2 + b_{26}^1 r'^2) \right] + w_{16}^1 \epsilon_{16}^1 S_l \left( -\frac{2}{3} c_{16}^1 \right) \exp \left[ -\frac{2}{3} (a_{16}^1 r^2 + b_{16}^1 r'^2) \right] \\ & + w_{56}^1 \epsilon_{56}^1 S_l \left( -\frac{2}{3} c_{56}^1 \right) \exp \left[ -\frac{2}{3} (a_{56}^1 r^2 + b_{56}^1 r'^2) \right] + w_{25}^1 \epsilon_{25}^1 S_l \left( -\frac{2}{3} c_{25}^1 \right) \exp \left[ -\frac{2}{3} (a_{25}^1 r^2 + b_{25}^1 r'^2) \right] \\ & \left. + w_{12}^1 \epsilon_{12}^1 S_l \left( -\frac{2}{3} c_{12}^1 \right) \exp \left[ -\frac{2}{3} (a_{12}^1 r^2 + b_{12}^1 r'^2) \right] \right\} \\ & + \epsilon_2 \left\{ w_{12}^2 \epsilon_{12}^2 S_l \left( -\frac{2}{3} c_{12}^2 \right) \exp \left[ -\frac{2}{3} (a_{12}^2 r^2 + b_{12}^2 r'^2) \right] + w_{56}^2 \epsilon_{56}^2 S_l \left( -\frac{2}{3} c_{56}^2 \right) \exp \left[ -\frac{2}{3} (a_{56}^2 r^2 + b_{56}^2 r'^2) \right] \right. \\ & + w_{34}^2 \epsilon_{34}^2 S_l \left( -\frac{2}{3} c_{34}^2 \right) \exp \left[ -\frac{2}{3} (a_{34}^2 r^2 + b_{34}^2 r'^2) \right] + w_{13}^2 \epsilon_{13}^2 S_l \left( -\frac{2}{3} c_{13}^2 \right) \exp \left[ -\frac{2}{3} (a_{13}^2 r^2 + b_{13}^2 r'^2) \right] \\ & \left. + w_{35}^2 \epsilon_{35}^2 S_l \left( -\frac{2}{3} c_{35}^2 \right) \exp \left[ -\frac{2}{3} (a_{35}^2 r^2 + b_{35}^2 r'^2) \right] + w_{15}^2 \epsilon_{15}^2 S_l \left( -\frac{2}{3} c_{15}^2 \right) \exp \left[ -\frac{2}{3} (a_{15}^2 r^2 + b_{15}^2 r'^2) \right] \right\}, \end{aligned} \quad (\text{A13})$$

and

$$\mathcal{G}_{pq} = 2\epsilon_1 S_l \left( -\frac{2}{3} c_1 \right) \exp \left[ -\frac{2}{3} (a_1 r^2 + b_1 r'^2) \right] - \epsilon_2 S_l \left( -\frac{2}{3} c_2 \right) \exp \left[ -\frac{2}{3} (a_2 r^2 + b_2 r'^2) \right]. \quad (\text{A14})$$

In the preceding three equations, the quantities  $S_i(\omega)$  and  $T_i(\omega)$  are given by

$$S_i(\omega) = \frac{4\pi}{\omega} \mathcal{J}_{i+1/2}(\omega r r'), \quad (\text{A15})$$

and

$$T_i(\omega) = \frac{4\pi}{\omega} \left[ \mathcal{J}_{i+3/2}(\omega r r') - \frac{l}{\omega r r'} \mathcal{J}_{i+1/2}(\omega r r') \right], \quad (\text{A16})$$

where  $\mathcal{J}(x)$  is a hyperbolic spherical Bessel function. Also, in the above equations, the following definitions have been made:

$$\begin{aligned} \epsilon_1 &= \left(\frac{4}{3}\right)^3 \left(\frac{\pi}{\alpha}\right)^3 \left(\frac{\pi}{4\alpha + 3\alpha_p + 3\alpha_q}\right)^{3/2}, \\ \epsilon_2 &= \left(\frac{4}{3}\right)^3 \left(\frac{\pi}{2\alpha}\right)^{3/2} \left(\frac{\pi}{\alpha + \alpha_p}\right)^{3/2} \left(\frac{\pi}{\alpha + \alpha_q}\right)^{3/2}, \\ a_1 &= \frac{d_1}{e_1}, \quad b_1 = \frac{f_1}{e_1}, \quad c_1 = \frac{g_1}{e_1}, \end{aligned}$$

with

$$\begin{aligned} d_1 &= 6\alpha^2 + \alpha(5\alpha_p + 17\alpha_q) + 6\alpha_p\alpha_q, \\ f_1 &= d_1 \quad \text{with } \alpha_p \leftrightarrow \alpha_q, \\ g_1 &= 12\alpha^2 + 4\alpha(\alpha_p + \alpha_q) + 12\alpha_p\alpha_q, \\ e_1 &= 12\alpha + 9(\alpha_p + \alpha_q), \\ a_2 &= b_2 = \frac{5}{3}\alpha, \quad c_2 = -\frac{8}{3}\alpha, \\ Q_a &= \frac{1}{3e_1^2} [288\alpha^4 + 96\alpha^3(4\alpha_p + 7\alpha_q) \\ &\quad + 8\alpha^2(20\alpha_p^2 + 112\alpha_p\alpha_q + 149\alpha_q^2) \\ &\quad + 16\alpha(6\alpha_p^2\alpha_q + 51\alpha_p\alpha_q^2) + 360\alpha_p^2\alpha_q^2], \\ Q_b &= Q_a \quad \text{with } \alpha_p \leftrightarrow \alpha_q, \\ Q_c &= \frac{1}{3e_1^2} [576\alpha^4 + 1056\alpha^3(\alpha_p + \alpha_q) \\ &\quad + 16\alpha^2(8\alpha_p^2 + 49\alpha_p\alpha_q + 8\alpha_q^2) \\ &\quad + 912\alpha(\alpha_p^2\alpha_q + \alpha_p\alpha_q^2) + 720\alpha_p^2\alpha_q^2], \\ w_{23}^1 &= 3w_k + 3m_k, \quad w_{15}^1 = w_k - 4m_k + 2b_k - 2h_k, \\ w_{26}^1 &= 3w_k - 2m_k + b_k - 3h_k, \quad w_{16}^1 = w_k + m_k + b_k + h_k, \\ w_{56}^1 &= w_{16}^1, \quad w_{25}^1 = 3w_k + 3m_k, \\ w_{12}^1 &= w_{25}^1, \quad w_{12}^2 = w_k + m_k + b_k + h_k, \\ w_{56}^2 &= w_{12}^2, \quad w_{34}^2 = w_{12}^2, \\ w_{13}^2 &= 4w_k + 4m_k - 2b_k - 2h_k, \quad w_{35}^2 = w_{13}^2, \\ w_{15}^2 &= 4w_k - 6m_k + 6b_k - 2h_k, \\ \epsilon_{23}^1 &= \left(\frac{\alpha}{\alpha + 2\kappa_k}\right)^{3/2}, \quad a_{23}^1 = a_1, \quad b_{23}^1 = b_1, \quad c_{23}^1 = c_1, \end{aligned}$$

$$\begin{aligned} \epsilon_{15}^1 &= 1, \quad a_{15}^1 = a_1 + \frac{8}{3}\kappa_k, \\ b_{15}^1 &= b_1 + \frac{8}{3}\kappa_k, \quad c_{15}^1 = c_1 + \frac{16}{3}\kappa_k, \\ \epsilon_{26}^1 &= \left[ \frac{\alpha e_1}{\alpha e_1 + 6\kappa_k(2\alpha + \alpha_p + \alpha_q)} \right]^{3/2}, \\ a_{26}^1 &= \frac{\alpha d_1 + 2\kappa_k[12\alpha^2 + 7\alpha(\alpha_p + \alpha_q) + 2\alpha_p\alpha_q]}{\alpha e_1 + 6\kappa_k(2\alpha + \alpha_p + \alpha_q)}, \\ b_{26}^1 &= \frac{\alpha f_1 + 2\kappa_k[12\alpha^2 + 7\alpha(\alpha_p + \alpha_q) + 2\alpha_p\alpha_q]}{\alpha e_1 + 6\kappa_k(2\alpha + \alpha_p + \alpha_q)}, \\ c_{26}^1 &= \frac{\alpha g_1 - 2\kappa_k[12\alpha^2 + 4\alpha(\alpha_p + \alpha_q) - 4\alpha_p\alpha_q]}{\alpha e_1 + 6\kappa_k(2\alpha + \alpha_p + \alpha_q)}, \\ \epsilon_{16}^1 &= \left(\frac{e_1}{e_1 + 36\kappa_k}\right)^{3/2}, \\ a_{16}^1 &= \frac{d_1 + \kappa_k(20\alpha + 24\alpha_q)}{e_1 + 36\kappa_k}, \\ b_{16}^1 &= \frac{f_1 + \kappa_k(68\alpha + 24\alpha_q)}{e_1 + 36\kappa_k}, \\ c_{16}^1 &= \frac{g_1 + \kappa_k(16\alpha + 48\alpha_q)}{e_1 + 36\kappa_k}, \\ \epsilon_{56}^1 &= \epsilon_{16}^1 \quad \text{with } \alpha_p \leftrightarrow \alpha_q, \\ a_{56}^1 &= b_{16}^1 \quad \text{with } \alpha_p \leftrightarrow \alpha_q, \\ b_{56}^1 &= a_{16}^1 \quad \text{with } \alpha_p \leftrightarrow \alpha_q, \\ c_{56}^1 &= c_{16}^1 \quad \text{with } \alpha_p \leftrightarrow \alpha_q, \\ \epsilon_{12}^1 &= \left[ \frac{\alpha e_1}{\alpha e_1 + 6\kappa_k(4\alpha + \alpha_p + \alpha_q)} \right]^{3/2}, \\ a_{12}^1 &= \frac{\alpha d_1 + 2\kappa_k(10\alpha^2 + 7\alpha\alpha_p + 27\alpha\alpha_q + 2\alpha_p\alpha_q)}{\alpha e_1 + 6\kappa_k(4\alpha + \alpha_p + \alpha_q)}, \\ b_{12}^1 &= \frac{\alpha f_1 + 2\kappa_k(10\alpha^2 + 7\alpha\alpha_p + 3\alpha\alpha_q + 2\alpha_p\alpha_q)}{\alpha e_1 + 6\kappa_k(4\alpha + \alpha_p + \alpha_q)}, \\ c_{12}^1 &= \frac{\alpha g_1 + 2\kappa_k(20\alpha^2 - 4\alpha\alpha_p + 12\alpha\alpha_q + 4\alpha_p\alpha_q)}{\alpha e_1 + 6\kappa_k(4\alpha + \alpha_p + \alpha_q)}, \\ \epsilon_{25}^1 &= \epsilon_{12}^1 \quad \text{with } \alpha_p \leftrightarrow \alpha_q, \\ a_{25}^1 &= b_{12}^1 \quad \text{with } \alpha_p \leftrightarrow \alpha_q, \\ b_{25}^1 &= a_{12}^1 \quad \text{with } \alpha_p \leftrightarrow \alpha_q, \\ c_{25}^1 &= c_{12}^1 \quad \text{with } \alpha_p \leftrightarrow \alpha_q, \\ \epsilon_{12}^2 &= \left(\frac{\alpha + \alpha_p}{\alpha + \alpha_p + 4\kappa_k}\right)^{3/2}, \quad a_{12}^2 = a_2, \\ b_{12}^2 &= b_2, \quad c_{12}^2 = c_2, \\ \epsilon_{56}^2 &= \left(\frac{\alpha + \alpha_q}{\alpha + \alpha_q + 4\kappa_k}\right)^{3/2}, \quad a_{56}^2 = a_2, \\ b_{56}^2 &= b_2, \quad c_{56}^2 = c_2, \\ \epsilon_{34}^2 &= \left(\frac{\alpha}{\alpha + 2\kappa_k}\right)^{3/2}, \quad a_{34}^2 = a_2, \end{aligned}$$

$$\begin{aligned}
b_{34}^2 &= b_2, & c_{34}^2 &= c_2, \\
\epsilon_{13}^2 &= \left[ \frac{6\alpha(\alpha + \alpha_p)}{6\alpha(\alpha + \alpha_p) + 3\kappa_k(3\alpha + \alpha_p)} \right]^{3/2}, & a_{13}^2 &= \frac{10\alpha^2(\alpha + \alpha_p) + \alpha\kappa_k(31\alpha + 21\alpha_p)}{6\alpha(\alpha + \alpha_p) + 3\kappa_k(3\alpha + \alpha_p)}, \\
b_{13}^2 &= \frac{10\alpha^2(\alpha + \alpha_p) + \alpha\kappa_k(19\alpha + 9\alpha_p)}{6\alpha(\alpha + \alpha_p) + 3\kappa_k(3\alpha + \alpha_p)}, & c_{13}^2 &= -\frac{16\alpha^2(\alpha + \alpha_p) + \alpha\kappa_k(40\alpha + 24\alpha_p)}{6\alpha(\alpha + \alpha_p) + 3\kappa_k(3\alpha + \alpha_p)}, \\
\epsilon_{35}^2 &= \epsilon_{13}^2 \quad \text{with } \alpha_p \leftrightarrow \alpha_q, & a_{35}^2 &= b_{13}^2 \quad \text{with } \alpha_p \leftrightarrow \alpha_q, \\
b_{35}^2 &= a_{13}^2 \quad \text{with } \alpha_p \leftrightarrow \alpha_q, & c_{35}^2 &= c_{13}^2 \quad \text{with } \alpha_p \leftrightarrow \alpha_q, \\
\epsilon_{15}^2 &= \left[ \frac{3(\alpha + \alpha_p)(\alpha + \alpha_q)}{3(\alpha + \alpha_p)(\alpha + \alpha_q) + 3\kappa_k(2\alpha + \alpha_p + \alpha_q)} \right]^{3/2}, & a_{15}^2 &= b_{15}^2 = \frac{5\alpha(\alpha + \alpha_p)(\alpha + \alpha_q) + \kappa_k[12\alpha^2 + 7\alpha(\alpha_p + \alpha_q) + 2\alpha_p\alpha_q]}{3(\alpha + \alpha_p)(\alpha + \alpha_q) + 3\kappa_k(2\alpha + \alpha_p + \alpha_q)}, \\
c_{15}^2 &= -\frac{8\alpha(\alpha + \alpha_p)(\alpha + \alpha_q) + \kappa_k[12\alpha^2 + 4\alpha(\alpha_p + \alpha_q) - 4\alpha_p\alpha_q]}{3(\alpha + \alpha_p)(\alpha + \alpha_q) + 3\kappa_k(2\alpha + \alpha_p + \alpha_q)}.
\end{aligned}$$

It should be noted that, as in our previous  $d + \alpha$  calculation,<sup>10</sup> we have neglected the exchange contribution in the Coulomb interaction.

#### APPENDIX B: COMPUTATION OF THE QUANTITIES IN THE DISTORTION KERNEL

Since the mathematical structure of the functions  $\Psi_0$  and  $\tilde{\chi}_{li}$  are similar, we can derive the quantity  $u_{li}(r)$  of Eq. (31) in a straightforward manner. It is of the form

$$u_{li}(r) = \eta_i \left\{ \left[ -\frac{\hbar^2}{2\mu} \left( \frac{d^2}{dr^2} - \frac{l(l+1)}{r^2} \right) - E_i + V_{Di}(r) + V_{Ci}(r) \right] g_{li}(r) + \int_0^\infty k_{li}(r, r') g_{li}(r') dr' \right\}. \quad (\text{B1})$$

In Eq. (B1), we have defined

$$\eta_i = \langle \phi_\alpha \phi_d \xi | \phi_\alpha \phi_i \xi \rangle_{\vec{r}} \quad (\text{B2})$$

and

$$E_i = E' - E_\alpha - E_{di}. \quad (\text{B3})$$

The quantities  $V_{Di}(r)$ ,  $V_{Ci}(r)$ ,  $k_{li}(r, r')$ , and  $E_{di}$  are obtained from the corresponding expressions in Appendix A with  $\alpha_q$  replaced by  $\tilde{\alpha}_i$ ,  $A_q$  replaced by 1, and no summation over the index  $q$ . For example,

$$\begin{aligned}
V_{Di}(r) &= -\frac{1}{G_i} \sum_{k=1}^2 V_{0k} w_{15}^0 \sum_{p=1}^3 A_p \left( \frac{\pi^3}{4\alpha^3} \right)^{3/2} \left( \frac{\pi}{\alpha_p + \tilde{\alpha}_i} \right)^{3/2} \left[ \frac{4\alpha(\alpha_p + \tilde{\alpha}_i)}{4\alpha(\alpha_p + \tilde{\alpha}_i) + \kappa_k(4\alpha + 3\alpha_p + 3\tilde{\alpha}_i)} \right]^{3/2} \\
&\quad \times \exp \left[ -\frac{4\alpha(\alpha_p + \tilde{\alpha}_i)\kappa_k}{4\alpha(\alpha_p + \tilde{\alpha}_i) + \kappa_k(4\alpha + 3\alpha_p + 3\tilde{\alpha}_i)} r^2 \right], \quad (\text{B4})
\end{aligned}$$

with

$$G_i = \sum_{p=1}^3 A_p \left( \frac{\pi^3}{4\alpha^3} \right)^{3/2} \left( \frac{\pi}{\alpha_p + \tilde{\alpha}_i} \right)^{3/2}. \quad (\text{B5})$$

In the computation of  $u_{li}(r)$  from Eq. (B1), the following relations are useful:

$$\mathcal{J}_\nu(x) = i^{\nu-1} (\frac{1}{2}\pi x)^{1/2} J_\nu(ix) \quad (\text{B6})$$

and

$$\int_0^\infty e^{-a^2 t^2} t^{\mu-1} J_\nu(bt) dt = \frac{\Gamma(\frac{1}{2}\mu + \frac{1}{2}\nu)}{2a^\mu \Gamma(\nu+1)} \left( \frac{b}{2a} \right)^\nu M \left( \frac{1}{2}\mu + \frac{1}{2}\nu, \nu+1, -\frac{b^2}{4a^2} \right) \quad [\text{Re}(\mu + \nu) > 0, \text{Re}a^2 > 0], \quad (\text{B7})$$

where  $J_\nu(x)$  is a Bessel function of the first kind,  $\Gamma(x)$  is a  $\gamma$  function, and  $M(a, b, z)$  is a confluent hypergeometric function.

The quantity  $\langle \chi_{li} | H | \tilde{\chi}_{lj} \rangle$  is also needed in the computation and can be calculated in a manner similar to

$u_{i,t}(r)$ . It is given by

$$\langle \chi_{i,t} | H | \bar{\chi}_{i,t} \rangle = \eta_{ij} \int_0^\infty g_{i,t}(r) \left\{ \left[ -\frac{\hbar^2}{2\mu} \left( \frac{d^2}{dr^2} - \frac{l(l+1)}{r^2} \right) - E_{ij} + V_{D,ij}(r) + V_{C,ij}(r) \right] g_{i,t}(r) + \int_0^\infty k_{i,ij}(r, r') g_{i,t}(r') dr' \right\} dr, \quad (\text{B8})$$

with

$$\eta_{ij} = \langle \phi_\alpha \phi_i \xi | \phi_\alpha \phi_j \xi \rangle^\dagger \quad (\text{B9})$$

and

$$E_{ij} = E' - E_\alpha - E_{d,ij}. \quad (\text{B10})$$

Here also,  $V_{D,ij}(r)$ ,  $V_{C,ij}(r)$ ,  $k_{i,ij}(r, r')$ , and  $E_{d,ij}$  are obtained from the corresponding expressions in Appendix A with  $\alpha_p$  replaced by  $\bar{\alpha}_i$ ,  $\alpha_q$  replaced by  $\bar{\alpha}_j$ ,  $A_p A_q$  replaced by 1, and no summation over the indices  $p$  and  $q$ . For example,  $V_{D,ij}$  is given by

$$V_{D,ij}(r) = -\frac{1}{G_{ij}} \sum_{k=1}^2 V_{0k} w_{1s}^0 \left( \frac{\pi^3}{4\alpha^3} \right)^{3/2} \left( \frac{\pi}{\bar{\alpha}_i + \bar{\alpha}_j} \right)^{3/2} \left[ \frac{4\alpha(\bar{\alpha}_i + \bar{\alpha}_j)}{4\alpha(\bar{\alpha}_i + \bar{\alpha}_j) + \kappa_k(4\alpha + 3\bar{\alpha}_i + 3\bar{\alpha}_j)} \right]^{3/2} \\ \times \exp \left[ -\frac{4\alpha(\bar{\alpha}_i + \bar{\alpha}_j)\kappa_k}{4\alpha(\bar{\alpha}_i + \bar{\alpha}_j) + \kappa_k(4\alpha + 3\bar{\alpha}_i + 3\bar{\alpha}_j)} r^2 \right], \quad (\text{B11})$$

with

$$G_{ij} = \left( \frac{\pi^3}{4\alpha^3} \right)^{3/2} \left( \frac{\pi}{\bar{\alpha}_i + \bar{\alpha}_j} \right)^{3/2}. \quad (\text{B12})$$

In the computation of  $\langle \chi_{i,t} | H | \bar{\chi}_{i,t} \rangle$ , the integration formula

$$\int_0^\infty e^{-st} t^{b-1} M(a, c, kt) dt \\ = \Gamma(b) s^{-b} F\left(a, b, c, \frac{k}{s}\right) \quad (|s| > |k|), \\ = \Gamma(b) (s-k)^{-b} F\left(c-a, b, c, \frac{k}{k-s}\right) \quad (|s-k| > |k|), \quad (\text{B13}) \\ [\text{Re}b > 0, \text{Re}s > \max(0, \text{Re}k)]$$

with  $F(a, b, c, z)$  being a hypergeometric function, has been used.

\* Work supported in part by the U.S. Atomic Energy Commission.

† A preliminary account of this work was presented at the American Physical Society, New York meeting, 1973 [Bull. Am. Phys. Soc. **18**, 21 (1973)].

<sup>1</sup>D. R. Thompson and Y. C. Tang, Phys. Rev. C **4**, 306 (1971), and references contained therein.

<sup>2</sup>D. R. Thompson, Y. C. Tang, and R. E. Brown, Phys. Rev. C **5**, 1939 (1972), and references contained therein.

<sup>3</sup>A. Herzenberg and A. S. Roberts, Nucl. Phys. **3**, 314 (1957).

<sup>4</sup>R. E. Brown and Y. C. Tang, Nucl. Phys. **A170**, 225 (1971).

<sup>5</sup>F. S. Chwieroth, R. E. Brown, Y. C. Tang, and D. R. Thompson, to be published.

<sup>6</sup>F. S. Chwieroth, Y. C. Tang, and D. R. Thompson, Nucl. Phys. **A189**, 1 (1972).

<sup>7</sup>L. C. Niem, P. Heiss, and H. H. Hackenbroich, Z. Phys. **244**, 346 (1971).

<sup>8</sup>H. Jacobs, K. Wildermuth, and E. Wurster, Phys. Lett. **29B**, 455 (1969).

<sup>9</sup>Y. C. Tang, K. Wildermuth, and L. D. Pearlstein, Phys. Rev. **123**, 548 (1961).

<sup>10</sup>D. R. Thompson and Y. C. Tang, Phys. Rev. **179**, 971 (1969).

<sup>11</sup>H. C. Benöhr and K. Wildermuth, Nucl. Phys. **A128**, 1 (1969).

<sup>12</sup>H. Feshbach, Ann. Phys. (N.Y.) **5**, 337 (1958); **19**, 287 (1962); **43**, 410 (1967).

<sup>13</sup>For the determination of an appropriate set of  $\tilde{\alpha}_i$  and  $\tilde{\beta}_i$  values, the choice of  $u$  is not critical. The value of 0.95 is chosen, simply because it is close to the value determined from  $\alpha+\alpha$  (Ref. 4) and  $p+\alpha$  (Ref. 2) scattering.

<sup>14</sup>The expectation values of the  $\alpha$ -particle Hamiltonian are equal to -26.61 and -31.66 MeV with  $\alpha$  equal to 0.514 and 0.80 fm<sup>-2</sup>, respectively.

<sup>15</sup>J. Schwager and E. W. Schmid, in *Proceedings of the International Conference on Few-Particle Problems in*

*Nuclear Physics, Los Angeles, California, 1972*, edited by I. Šlaus *et al.* (North-Holland, Amsterdam, 1973).

- <sup>16</sup>All energies will be in the c.m. system, unless otherwise stated.
- <sup>17</sup>L. C. McIntyre and W. Haeberli, Nucl. Phys. A91, 382 (1967).
- <sup>18</sup>P. Darriulat, D. Garreta, A. Tarrats, and J. Arvieux, Nucl. Phys. A94, 653 (1967).
- <sup>19</sup>J. A. Koepke, R. E. Brown, Y. C. Tang, and D. R. Thompson, to be published.
- <sup>20</sup>B. Tatischeff and I. Brissand, Nucl. Phys. A155, 89 (1970).